Zhao, J. & Guo, N. (2013). *Géotechnique* **63**, No. 8, 695–704 [http://dx.doi.org/10.1680/geot.12.P.040]

Unique critical state characteristics in granular media considering fabric anisotropy

J. ZHAO* and N. GUO*

The concept of the critical state in granular soils needs to make proper reference to the fabric structure that develops at critical state. This study identifies a unique property associated with the fabric structure relative to the stresses at critical state. A unique relationship between the mean effective stress and a fabric anisotropy parameter, K, defined by the first joint invariant of the deviatoric stress tensor and the deviatoric fabric tensor, is found at critical state, and is path-independent. Numerical simulations using the discrete-element method under different loading conditions and intermediate principal stress ratios identify a unique power law for this relationship. Based on the findings, a new definition of critical state for granular media is proposed. In addition to the conditions of constant stress and unique void ratio required by the conventional critical state concept, the new definition imposes the additional constraint that K reaches a unique value at critical state. A unique spatial critical state curve in the three-dimensional space K–e–p' is found for a granular medium, the projection of which onto the e–p' plane turns out to be the conventional critical state line. The new critical state concept provides an important reference state for a soil to reach, based on which the key concepts in the constitutive modelling of granular media, including the choice of state parameters, dilatancy relation and non-coaxiality, are reassessed, and future exploratory topics are discussed.

KEYWORDS: anisotropy; discrete-element modelling; fabric/structure of soils; plasticity

INTRODUCTION

The critical state theory (CST) developed by Roscoe *et al.* (1958) and Schofield & Wroth (1968) laid the foundation for critical state soil mechanics. Fundamental to the theory is the concept of critical state that identifies an ultimate state for a soil to converge under sustained shear. Critical state in granular soils refers to a state of continuous shear deformation with a constant volume under constant stress. In essence, at critical state, a soil may reach a constant stress ratio $\eta = q/p' = M$ (where p' and q are the commonly referred mean effective stress and the deviatoric stress respectively, and M denotes a material coefficient that may depend on the shear mode – for example, the Lode angle or intermediate principal stress ratio – and a unique critical void ratio e_c. The classical definition of critical state emphasises *fabric isotropy* (the void ratio), but lacks a proper reference to *fabric anisotropy*. Experimental and numerical studies have indicated that the behaviour of a granular soil under shear is predominantly anisotropic. Under sustained shear, the induced plastic flow deformation will mobilise particles in a granular assembly to adjust themselves by sliding and rolling to provide better support for the external load, which naturally leads to the formation of an anisotropic fabric structure to serve this role optimally. The anisotropic fabric structure evolves steadily with the loading process. Indeed, early micromechanical studies suggested that the macroscopic strength of a granular material is strongly correlated with the degree of anisotropy in the fabric structure during almost all stages of the loading history (e.g. Rothenburg & Bathurst, 1989). It has been shown that the anisotropic fabric structure sustains the majority of the applied deviatoric stress, and provides the apparent shear strength for soils (e.g. in terms of the stress ratio). Meanwhile, experimental data have also proved that the soil response can be highly anisotropic prior to the critical state (Nakata *et al.*, 1998; Yoshimine *et al.*, 1998). Later micromechanical studies further verified that the soil fabric at critical state exhibits a clear anisotropic structure (e.g. Oda, 1972a, 1972b; Masson & Martinez, 2001; Li & Li, 2009).

The same observation was recently confirmed by the present authors through a series of numerical tests on granular media using the discrete-element method (DEM) (Guo & Zhao, 2013). Granular assemblies with different initial conditions were sheared under drained or undrained triaxial compression conditions. With the exception of some liquefied cases, the critical state was reached in all samples, unambiguously accompanied by a highly anisotropic fabric structure, irrespective of the initial conditions and loading conditions. Fig. 1 shows an example of the critical fabric structure found in a medium-dense sample. After the sample was sheared to an axial strain of around 44% (marked by a star in Fig. 1(a)), the soil reached a steady state that satisfied all necessary conditions according to the classic definition of a critical state. Meanwhile, a steadily flowing fabric structure can be observed in the sample, the key characteristics of which remain largely unchanged with further development of shear deformation. Fig. 1(b) presents a visualisation of the fabric structure, showing the interparticle contacts and the formation of a contact force network. Each column in the figure physically denotes a directional interparticle contact, the thickness of which represents the relative magnitude of the normal contact force at the contact. It is evident that such a critical fabric structure is highly anisotropic, with the major anisotropic orientation aligning with the loading direction (the deviatoric stress direction, shown in Fig. 1(b)). Extraction of the statistical characteristics of the critical fabric structure from the simulated data further confirmed that it can only be described by an anisotropic-tensor-valued

Manuscript received 21 March 2012; revised manuscript accepted 28 November 2012. Published online ahead of print 12 February 2013. Discussion on this paper closes on 1 November 2013, for further details see p. ii.

* Hong Kong University of Science and Technology, Clearwater Bay, Kowloon, Hong Kong.

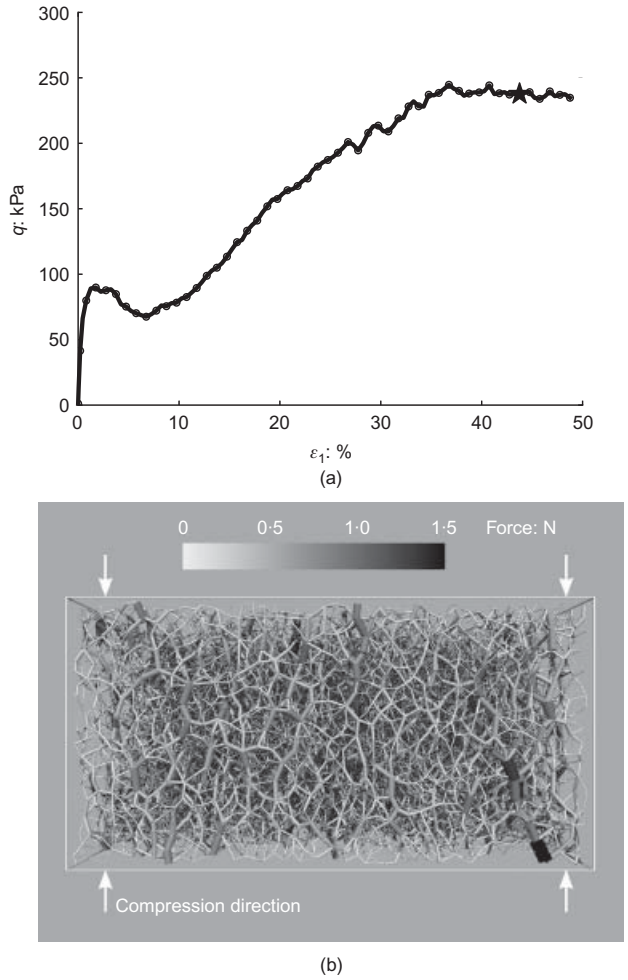

Fig. 1. Typical medium-dense sand sample subjected to undrained shear towards critical state by DEM simulation: (a) stress–strain relation; (b) fabric structure in terms of contact force chain network attained at critical state

quantity. A scalar-valued critical void ratio e_c alone cannot adequately represent the complete picture. Indeed, when proposing their *isotropic* state parameter ψ $(= e - e_c)$, Been & Jefferies (1985) suggested that the critical state in soil may be (anisotropic) fabric dependent. They further emphasised the important effect of the soil fabric on the overall behaviour of the granular medium (e.g. the soil dilatancy). More recent experimental data have shown that the dilatancy of soil is profoundly influenced by either a fixed or variable loading direction relative to the orientation of the specimen, in which fabric anisotropy is believed to play a pivotal role (e.g. Verdugo & Ishihara, 1996; Yoshimine *et al.*, 1998). Evidently, there is a missing link in the classic concept of critical state that prevents it from characterising the actual behaviour of soil in a critical state in a manner that is both physically realistic and mathematically comprehensive.

The present study was motivated by the anisotropic critical state theory (ACST) recently proposed by Li & Dafalias (2012). The ACST is based on the classic CST with proper inclusion of fabric anisotropy and fabric evolution. It offers a consistent theoretical framework for the future development of constitutive models for granular media. However, elegant as it may be, the ACST proves to be a highly idealised conceptual framework. The development of the theory was based on limited observations from two-dimensional DEM simulations (e.g. those reported by Li & Li (2009)). A number of important underlying assumptions, particularly those relevant to the characteristics of critical fabric anisotropy, still need rigorous verification. Although there has been significant progress in the development of advanced experimental techniques for probing the grain-scale information in granular media, such as X-ray micro-tomography and MRI imaging (Ng *et al.*, 1997; Mueth *et al.*, 2000; Hall *et al.*, 2010; Hasan & Alshibli, 2010, 2012), it remains a great practical challenge for experimenters to effectively explore and accurately quantify the intricate characteristics of the fabric structure in granular media at the particle scale, particularly when in a critical state. Numerical tools are the primary option for conducting such investigations: for instance, direct simulation of the grain system is possible using the DEM. Although not perfect, the DEM may help to extract useful information on the grain scale, including information relevant to the fabric structure at critical state. In this paper, a three-dimensional DEM is used to explore the signature properties of the critical state in a granular material by taking the critical fabric anisotropy into consideration.

METHODOLOGY AND APPROACH

Sample preparation and loading paths

The three-dimensional DEM code used in this study uses a linear force–displacement contact law in conjunction with Coulomb's friction law, which governs the sliding friction (Abe *et al.*, 2004; Guo & Zhao, 2013). The normal stiffness and tangential stiffness are set to be $k_n/r = k_s/r = 100$ MPa, where r denotes the equivalent radius of two contacted particles. The interparticle friction coefficient in Coulomb's law adopts the value $\mu = 0{\cdot}5$, which is typical for quartz sand. Around 32 000 polydisperse spherical particles with radii ranging from 0·2 mm to 0·6 mm are randomly generated in a cubic container with rigid frictionless walls. The particle-size distribution of an assembly is approximated to that of Toyoura sand (see Guo & Zhao (2013) for a detailed description of the approximating method). Special techniques for staged isotropic consolidation have been developed to produce random assemblies with different initial void ratios (Guo & Zhao, 2013). As all particles are randomly generated and isotropically consolidated, the influence of the initial fabric anisotropy on the shear response is excluded from consideration (the significance of which will be discussed later). All obtained samples are then monotonically sheared in two loading conditions (drained and undrained), which are commonly treated in soil mechanics. To conduct the tests in the drained condition, the horizontal pressures on the four vertical walls of the cube are kept constant during the shear using a servo-control technique. In the undrained tests, only dry particles are considered: hence the undrained condition is simulated in an approximate sense by imposing a constant-volume constraint on the sheared sample (see also Yimsiri & Soga (2010)). During the undrained shear, the horizontal strain is continuously adjusted according to the applied vertical compressive force, while the total volume of the assembly is maintained constant. To investigate the influence of the loading path on the final observations, various constant-b tests (see also Barreto & O'Sullivan (2012)) have been explored, where $b = (\sigma_2 - \sigma_3)/(\sigma_1 - \sigma_3)$ is the intermediate principal stress ratio. Five different cases of b were investigated: $b = 0$, 0·25, 0·5, 0·75 and 1. Notably, $b = 0$ and $b = 1$ correspond to conventional triaxial compression and triaxial extension respectively. To gain more confidence in the final data, some supplementary constant-p' tests were also conducted.

Stress tensor and fabric tensor

The following definition of a stress tensor proposed by Christoffersen *et al.* (1981) is applied to quantify the macroscopic response of a DEM assembly.

$$\sigma_{ij} = \frac{1}{V}\sum_{c\in N_c} f_i^c d_j^c \tag{1}$$

where V is the total volume of the assembly, N_c is the total number of contacts, $\boldsymbol{f}^c$ denotes the contact force at a contact, and $\boldsymbol{d}^c$ defines the branch vector joining the centres of two contacted particles. The mean effective stress and deviatoric stress can then be determined by $p' = \sigma_{ii}/3$ and $q = \sqrt{3 s_{ij} s_{ij}/2}$, where $s_{ij} = \sigma_{ij} - \delta_{ij} p'$ (δ_{ij} is the Kronecker delta). As the treatment involves cubic samples confined by rigid walls, the axial strain and the volumetric strain can be approximately defined by the displacement of the boundary walls.

To characterise the fabric structure, a suitable variable is needed to quantify the fabric anisotropy. Among the various definitions of fabric tensor (e.g. Oda, 1972a, 1982; Satake, 1982; Kanatani, 1984; Baji, 1996; Li & Li, 2009), the *contact-normal-based* proposition by Satake (1982) and Oda (1982) is chosen here.

$$\phi_{ij} = \int_{\Theta} E(\Theta) n_i n_j \mathrm{d}\Theta \tag{2}$$

where $\boldsymbol{n}$ is the unit vector along the normal direction of the contact plane; Θ characterises the orientation of $\boldsymbol{n}$ relative to the global coordination system; and $E(\Theta)$ is the distribution probability density function (PDF). In most cases it is sufficient to apply the second-order Fourier expansion of $E(\Theta)$ to characterise the contact normals (Ouadfel & Rothenburg, 2001),

$$E(\Theta) = \frac{1}{4\pi}(1 + F_{ij} n_i n_j) \tag{3}$$

where the second-order anisotropic fabric tensor $F_{ij} = 15/2(\phi_{ij} - 1/3\delta_{ij})$ is deviatoric and symmetric, and can be used to characterise the fabric anisotropy in the assembly. In practice, ϕ_{ij} (and hence F_{ij}) can be estimated from the discrete data of a granular assembly by

$$\phi_{ij} = \frac{1}{N_c}\sum_{c\in N_c} n_i^c n_j^c$$

where $\boldsymbol{n}^c$ denotes the unit contact normal vector.

Joint invariants of the stress tensor and the fabric tensor

Owing to the deviatoric nature of F_{ij}, its three invariants can be defined as follows.

$$\begin{aligned} J_1^F &= F_{ii} = 0 \\ J_2^F &= \tfrac{1}{2} F_{ij} F_{ji} \\ J_3^F &= \tfrac{1}{3} F_{ij} F_{jk} F_{ki} \end{aligned} \tag{4}$$

According to the representation theory (Wang, 1970; Spencer, 1971), any scalar-valued isotropic function of two second-order tensors can be expressed in terms of their own invariants together with *up to* four irreducible joint invariants between them. Consider the stress tensor defined in equation (1) and the fabric tensor F_{ij}; a scalar-valued function f of the two tensors can be expressed as

$$\begin{aligned} f &= f(\sigma_{ij}, F_{ij}) \\ &= f(I_1, J_{2D}, J_{3D}, J_1^F, J_2^F, J_3^F, K_1, K_2, K_3, K_4) \end{aligned} \tag{5}$$

where I_1, J_{2D}, J_{3D} are respectively the first invariant of the stress tensor and the second and third invariants of the deviatoric stress tensor s_{ij}. K_i ($i = 1, 2, 3, 4$) denotes the four joint invariants between the deviatoric stress tensor and the fabric tensor, given by

$$\begin{aligned} K_1 &= K = s_{ij} F_{ji} \\ K_2 &= s_{ij} F_{jk} F_{ki} \\ K_3 &= s_{ik} s_{kj} F_{ji} \\ K_4 &= s_{ik} s_{kj} F_{jl} F_{li} \end{aligned} \tag{6}$$

In the following, the first joint invariant K_1 is replaced by K for convenience.

RESULTS AND OBSERVATIONS

Over 80 numerical samples were sheared from different initial states (i.e. in terms of density and initial confining pressure) to a critical state under various monotonic loading paths. In our numerical simulations, all samples were found to reach a relatively steady state with constant stress and constant volume beyond an axial strain level of around 40%, which satisfies the classic description of a critical state. The soil state beyond this point is regarded as a critical state. Nevertheless, there are certain degrees of fluctuation in the soil response after this strain level. To minimise possible deviations caused by fluctuations, the relevant quantities (e.g. F_c, K_c) were averaged over a sustained stage of deformation, for example for an axial strain level ranging between 40% and 50%. The averaging technique appeared to be fairly effective, and led to relatively stable and consistent quantifications of critical states.

Critical void ratio

The critical void ratio was correlated with the mean effective stress p' for all samples under investigation, as shown in Fig. 2. All data points were found to collapse to the following general form (cf. Li, 1997; Li *et al.*, 1999).

$$e_c = e_\Gamma - \lambda_e \left(\frac{p'}{p_a}\right)^{\xi} \tag{7}$$

where e_Γ denotes the critical void ratio at $p' = 0$, λ_e and ξ are material constants, and $p_a = 101$ kPa is the atmospheric pressure. Our simulated data fit the expression in equation (7) well with $e_\Gamma = 0{\cdot}663$, $\lambda_e = 0{\cdot}008$ and $\xi = 1{\cdot}0$, which represents a linear relation. (The data are presented in Fig. 2 in a semi-log scale rather than a natural scale to render the

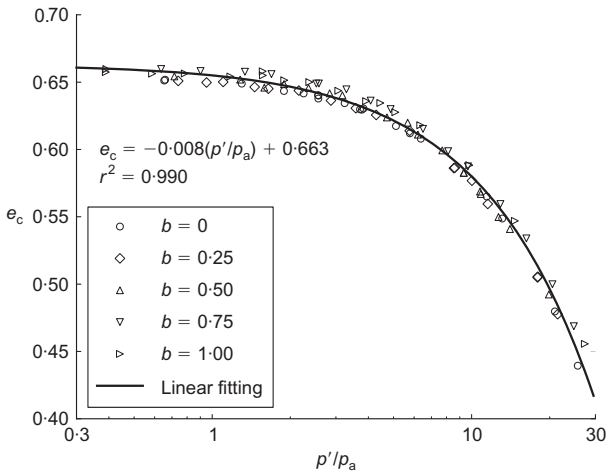

Fig. 2. Linear relation between critical void ratio and mean effective stress

data points in an even distribution over the chosen stress range.) Notably, a similar linear relationship was previously reported by Been *et al.* (1991) for Erksak sand, and by Ishihara (1993) for Toyoura sand. Note that the loading paths (e.g. with varying b), do not affect the above relationship. Evidently, the study identifies a unique critical state line in the e–p' plane for sand, which appears to support the general view taken by Been *et al.* (1991) and Ishihara (1993) on the uniqueness of the CSL (see also Jefferies & Been, 2006).

Critical fabric anisotropy

It is interesting to examine whether similar unique features can be identified for fabric anisotropy at critical state. The second invariant of F_{ij}^{c}

$$F_c = \sqrt{3F_{ij}^{c}F_{ij}^{c}/2}$$

is first selected to represent the degree of critical fabric anisotropy. The correlation between F_c and p' at critical state is plotted in Fig. 3. Interestingly, for each individual case of b, a power-law dependence of F_c on the critical mean effective stress p' is observed (cf. Guo & Zhao (2013) for the triaxial compression cases)

$$F_c = m_F\left(\frac{p'}{p_a}\right)^{\zeta} \tag{8}$$

where m_F denotes a parameter dependent on the Lode angle or b (e.g. $m_F = \hat{m}_F(b)$). The numerical results indicate $\zeta = -0{\cdot}14$ to $-0{\cdot}09$ for $b \in [0, 1]$. Evidently, according to the present definition of 'fabric tensor', a unique critical fabric structure independent of the loading path is not attainable.

Although not presented here, the third invariant of F_{ij} in a critical state, J_3^F, was also found to be non-unique. To explore whether the invariant functions of the three invariants lead to unique characterisations, the following function, which borrows the form of Lade's failure criterion, was also examined (cf. Thornton, 2000; Thornton & Zhang, 2010).

$$\eta^* = \frac{(I_1^F)^3}{2I_1^F I_2^F - 3I_3^F} \tag{9}$$

where I_i^F ($i = 1, 2, 3$) are the three invariants of the original fabric tensor ϕ_{ij} (not F_{ij}). Using this newly defined η^*, the results of various constant-b cases in critical states are replotted in Fig. 4. Although the use of an invariant function in the form of equation (9) considerably reduces the range of variation for all data, it still cannot unify all cases uniquely. Several different forms of invariant function (e.g. the Matsuoka–Nakai criterion-like invariant) were tried, and the observations are more or less similar to η^*. The examination using the usual measures of fabric tensor, as shown above, suggests that the critical fabric structure in a granular material is not unique (or loading path dependent).

Joint invariants at critical state

The property of critical fabric anisotropy is not unique. Meanwhile, it is known that the critical stress ratio (e.g. q/p') varies with the loading path. As shown by several past studies, the fabric anisotropy is intimately related to the stress state (e.g. Oda *et al.*, 1985; Thornton & Zhang, 2010). Hence it is inappropriate to quantify their critical state properties separately. In this case, the joint invariants of the two tensors may offer a more accurate characterisation of a soil in a critical state. To verify this, in Figs 5 and 6 the correlations are plotted between the two joint invariants K and K_2 defined in equations (6) with p' at critical state. The correlations between the third and the fourth joint invariants, K_3 and K_4, and p' exhibit trends similar to those of the second and first joint invariants respectively, which are not presented here. The correlation between K and p' is presented comparatively in both a natural scale and a log–log scale in Fig. 5. A striking observation is that the K value at critical state, K_c, can be uniquely correlated with the critical mean effective stress p' by the following power law

$$K_c = 0{\cdot}41p'^{0{\cdot}894} \tag{10}$$

Considering the great variety of sands, a more general power law may be postulated

$$K_c = \alpha p'^{\varsigma} \tag{11}$$

where α and ς are material constants. In contrast to the case of K, the correlation between K_2 (or K_3) and p' at critical state, as shown in Fig. 6, demonstrates a clear path-dependent feature. Consequently, K_c appears to be a better indicator of the compatibility of the critical stress with the fabric structure, and may be adopted to characterise the unique property of the critical state.

Based on equation (6), a pure measure of the relative orientation of the two tensors, A', can be further defined:

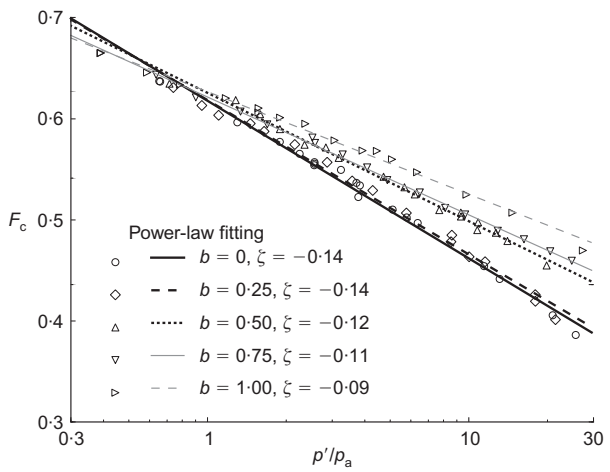

Fig. 3. Correlation between critical fabric anisotropy and mean effective stress

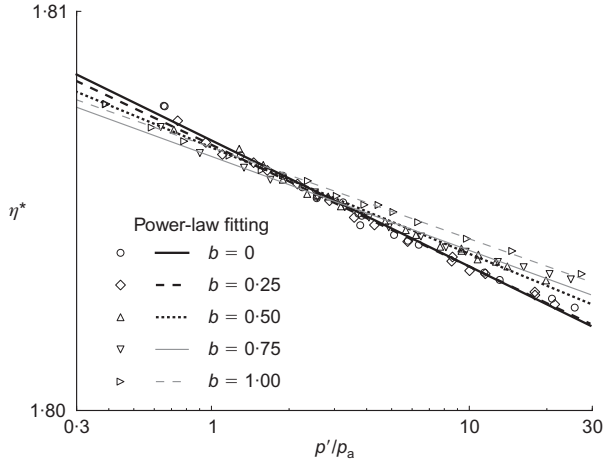

Fig. 4. Lade-failure-criterion-like scalar function of invariants of ϕ_{ij} at critical state against critical mean effective stress ($\eta^* = 1{\cdot}8$ corresponds to an isotropic state)

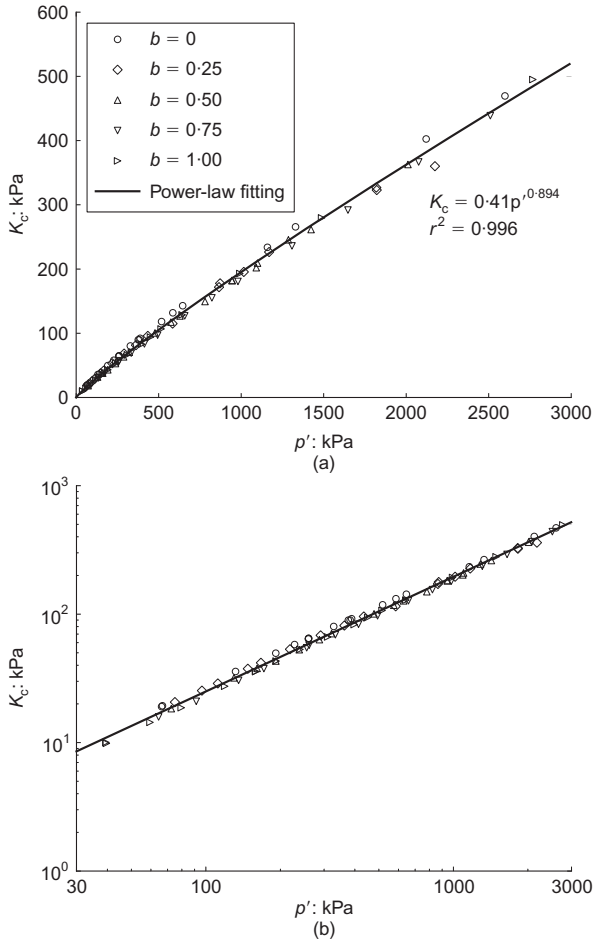

Fig. 5. Correlation between first joint invariant K and p' at critical state by power-law fitting: (a) natural scale; (b) log–log plot

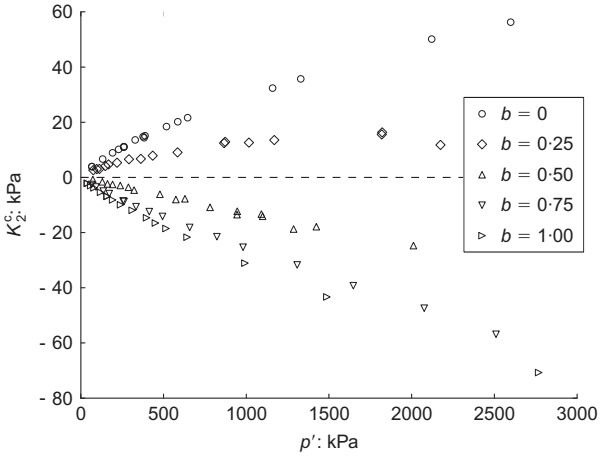

Fig. 6. Correlation of second joint invariant K_2 at critical state with p'

that is, $A' = n_{ij}^{\mathrm{F}} n_{ij}^{\mathrm{s}}$, where n_{ij}^{s} denotes the deviatoric stress direction and n_{ij}^{F} is the fabric direction. Note that A' is indeed a normalised quantity of the anisotropic variable A, as defined in Li & Dafalias (2012). The evolution of A' during the shearing process for five samples with different b is shown in Fig. 7. As shown, the stress and the fabric tensor tend to become coaxial quickly upon shear, and A' always approaches unity or a value very close to unity shortly after the application of shear, and then stays at this

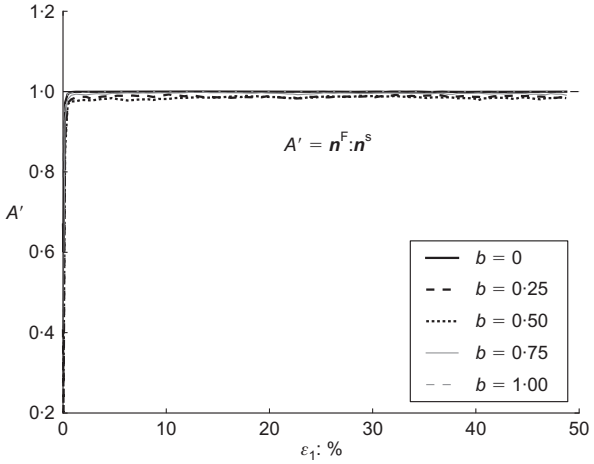

Fig. 7. Evolution of A' (relative orientation between fabric direction and stress direction) during shearing process towards critical state at various b

value before reaching the critical state. The observation provides clear evidence that the coaxiality of the deviatoric stress and the fabric anisotropy is indeed a very special property of the critical fabric structure, which is consistent with Li & Dafalias (2012).

State surface of K_c *in the deviatoric plane*

The above observation can be further verified by visualising the state surfaces for the various quantities concerned at critical state. This is inspired by the study conducted by Thornton & Zhang (2010). Following their approach, the state surfaces for both the critical state stresses and the critical fabric anisotropy are plotted in a three-dimensional deviatoric plane, in a manner analogous to that for a failure criterion. Fig. 8(a) shows the critical stress surface and critical fabric surface in the deviatoric plane obtained by different constant-b tests at a pressure level of around 1000 kPa. It is clearly observable that the critical state stresses form a smooth triangular-shaped surface, reminiscent of a Lade's criterion surface, whereas the critical fabric anisotropies form a surface with an inverted smoothed triangular shape, reciprocal to that of the critical state stresses. Thornton & Zhang (2010) observed similar behaviour for these quantities during the loading course of a granular assembly en route to a critical state. Yimsiri & Soga (2010) also observed a larger final fabric anisotropy under triaxial extension than under triaxial compression, which is consistent with the current authors' observation in Fig. 8(a).

Evidently, neither the critical state stress nor the critical fabric anisotropy has a circular state surface in the deviatoric plane, which explains their dependence on the loading path. Nevertheless, noting the complementary nature of the two surfaces, it is apparent that proper combinations of the two may lead to a circular state shape. The definition in equation (6) for the first (or the fourth) joint invariant offers one such combination. A further plot of K_c indeed confirms this expectation. As shown in Fig. 8(b), K_c does display a well-rounded circular shape in the deviatoric plane, which is independent of the Lode angle. This feature renders it suitable for use as a reference state for soil state characterisation.

The changes in the size and shape of the critical state yield surface, fabric anisotropy and K_c at six pressure levels (80 kPa, 300 kPa, 500 kPa, 700 kPa, 1000 kPa and 2000 kPa) are further plotted in Fig. 9. As shown in Figs 9(a) and 9(b),

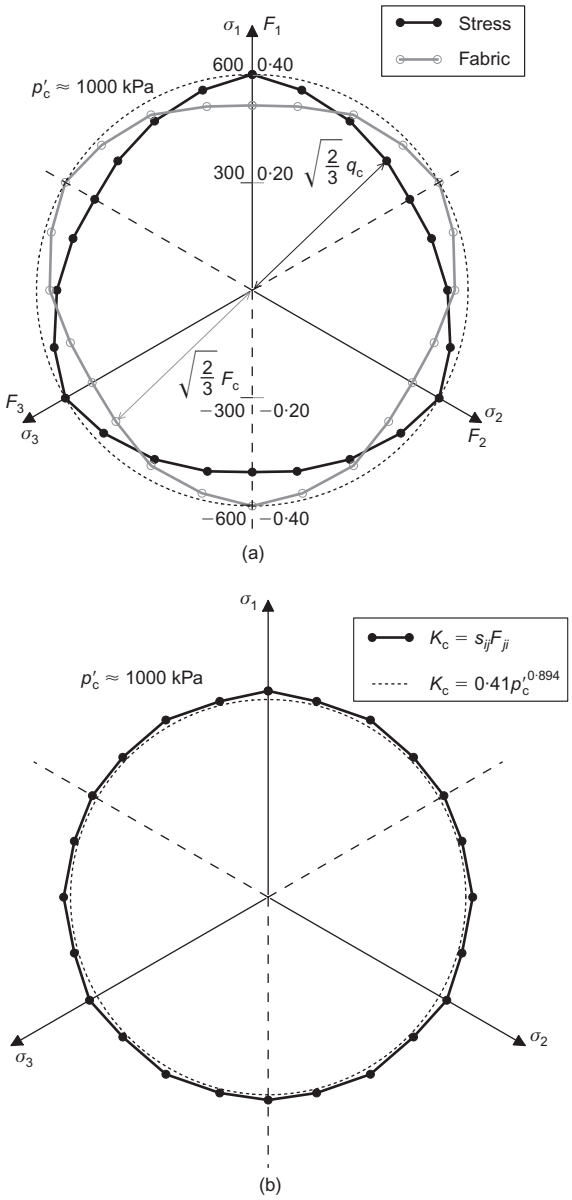

Fig. 8. State surfaces of: (a) critical state stress and critical fabric anisotropy in deviatoric plane; (b) K_c in deviatoric plane (at $p'_c \approx 1000$ kPa)

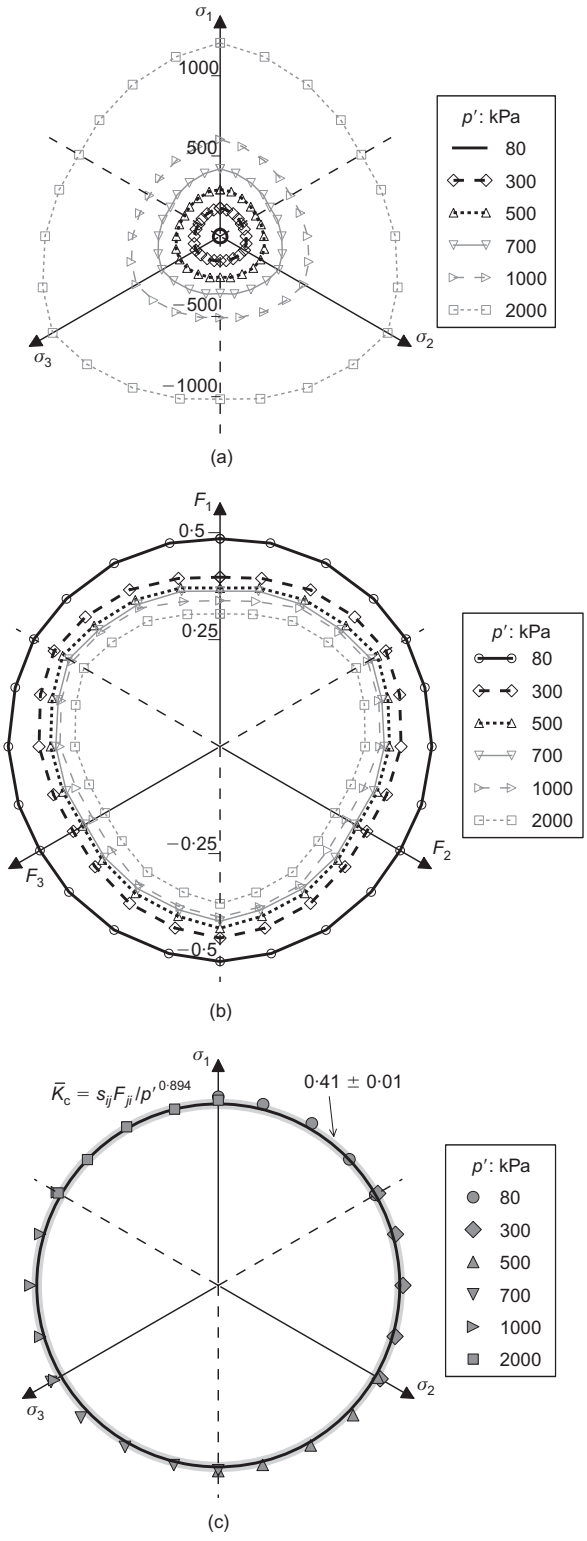

Fig. 9. Comparison of (a) critical state yield surfaces, (b) state surface for fabric anisotropy and (c) normalised K_c at various critical pressures

lower pressure levels lead to apparently smaller critical state yield surfaces, whereas the corresponding state surfaces for critical fabric anisotropy appear to be larger. Although the shapes of the critical state yield surface and the fabric anisotropy at each pressure level generally resemble those at $p'_c \approx 1000$ kPa, at lower pressures (e.g. $p'_c \approx 80$ kPa) both the critical state yield surface and the state surface for F_c are more rounded than they appear to be at higher pressures. In particular, if $r_M = M_c/M_e$ denotes the ratio between the critical stress ratios under triaxial compression and triaxial extension, it is evident from Fig. 9(a) that this ratio increases from around 1 to 1·2 when the critical pressure increases from 80 kPa to 2000 kPa. This ratio appears to be less sensitive to pressure in the low-pressure regime, but seems to become more sensitive when the pressure is high. A similarly defined ratio for F_c demonstrates a similar trend, except that it decreases from 1 to around 0·84 as the pressure increases (see Fig. 8(b)). In contrast, in all cases K_c is found to be a circle similar to that in Fig. 8(b), albeit with different radii. If a normalised measure, $\bar{K}_c = K_c/p'^{0{\cdot}894}_c$, is further defined to rescale the data, all surfaces of $\bar{K}_c$ are found to collapse approximately to a circle $\bar{K}_c = \text{constant}$ (around $0{\cdot}41 \pm 0{\cdot}01$ from the obtained data), as shown in Fig. 9(c), albeit with some minor deviations.

Unique critical state curve in K_c–e_c–p'_c *space*

In view of the observed unique dependence of both e_c and K_c on p'_c, it is evident that the three quantities are indeed

intercorrelated in a unique manner. The unique relationship is presented in the form of a spatial curve in K_c–e_c–p'_c space, as shown in Fig. 10. The two critical lines in Figs 2 and 5 are its projections in the e_c–p'_c plane and K_c–p'_c planes respectively. This new critical state curve nicely unifies the classic critical state concept with the case of fabric anisotropy. Note that the critical state line in e–p'–q space presented by Roscoe *et al.* (1963) (Fig. 6 therein) is indeed a special case of our critical state line when $F_c \equiv 1$ and $A' = 1$.

DISCUSSION AND OUTLOOK

It is instructive to discuss the significance of these new findings for some fundamental concepts and methodologies in theoretical soil mechanics. Only a brief discussion is devoted to each topic, owing to space limitations.

Critical state conditions

It is clear from the obtained findings that a complete picture of the critical state for granular materials needs to consider both the unique isotropic characteristics of the critical state and the critical fabric structure relevant to the critical stress. Following a method similar to that of Li & Dafalias (2012), a third condition on the anisotropic variable K is introduced into the classic critical state concept to furnish a new definition of anisotropic critical state as

$$\eta = \eta_c = \frac{q_c}{p'_c} = M(b)$$
$$e = e_c = \hat{e}_c(p') \tag{12}$$
$$K = K_c = \hat{K}_c(p')$$

Although the specific loading and fabric evolution law may be path dependent, the critical state conditions in equation (12) set a unique ultimate goal (or compass) for both the fabric isotropy and fabric anisotropy to converge with the applied shear stress, regardless of which loading paths are followed.

Anisotropic state parameter

The isotropic state parameter defined by Been & Jefferies (1985), $\psi = e - e_c$, reflects at best an isotropic soil state, which requires additional reference to the state of the fabric anisotropy. Based on the unique property shown by K_c, the following pair of state parameters is proposed to characterise the state in sand (note that $K_c > 0$)

$$\psi = e - e_c$$
$$\phi = \frac{K}{K_c} \tag{13}$$

Evidently, the critical state values for the two state parameters are $\psi = 0$, $\phi = 1$. To evaluate ϕ, it is important to recognise that the critical K_c might not necessarily be a maximum. Equation (13) borrows the definitions of ψ_A and ζ from Li & Dafalias (2012) (equations (12)–(15) therein).

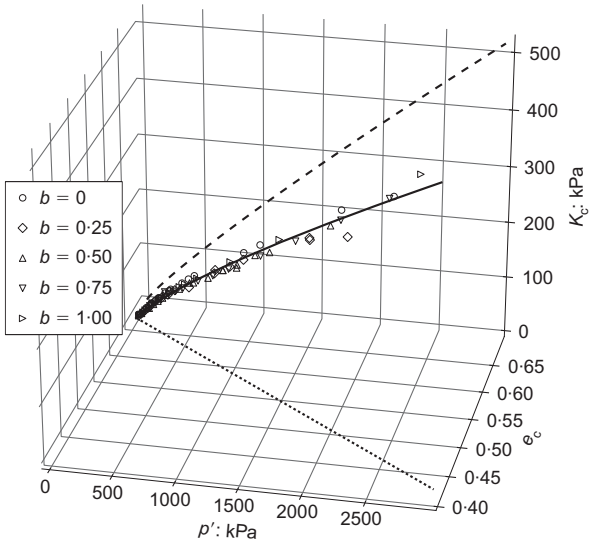

Fig. 10. Unique critical state curve plotted in K_c–e_c–p'_c space

Stress dilatancy

The experimental data indicate that the dilatancy of sand is influenced by fabric anisotropy. With the help of the state parameters defined in equation (13), the following state-dependent dilatancy relationship is suggested (cf. Li & Dafalias, 2000)

$$D = \hat{D}(\psi, \phi, \eta, C) \tag{14}$$

where C denotes a collection of intrinsic material constants. There may be more than one way to define the specific form of D. A specific example is demonstrated here. Assume an additive form of the state parameters defined in equation (13)

$$\theta = \psi + k[1 - (\boldsymbol{n}^L : \boldsymbol{n}^F)\phi] \tag{15}$$

where k is a material constant, and $\boldsymbol{n}^L$ is a unit tensor denoting the loading direction (e.g. the plastic strain rate direction; Li & Dafalias, 2012). The following general dilatancy relation may be proposed

$$D = \hat{D}[X(\theta) - Y(\eta)] \tag{16}$$

where X and Y are scalar-valued functions of θ and η respectively. A modified form of D from the expression in Li & Dafalias (2012) may be suggested

$$D = d(M\mathrm{e}^{m\theta} - \eta) \tag{17}$$

where m and d are positive material constants. The following observations are apparent from equation (17) (cf. Li & Dafalias, 2012).

(*a*) At critical state, $\psi = 0$ and $\phi = 1$, $\theta = 0$, $\eta = M$: thus $D = 0$.
(*b*) During flow liquefaction, θ approaches 0 and $\eta = M$, so that $D = 0$. However, as $\psi \neq 0$ and $\phi \neq 1$, it differs essentially from the critical state.
(*c*) The attainability of the phase transformation state as defined by Ishihara *et al.* (1975) for different sands can be easily explained, with D jointly controlled by ϕ and θ as well as by η.
(*d*) When the loading direction changes so abruptly (e.g. from $\boldsymbol{n}^L$ to $-\boldsymbol{n}^L$) that both the fabric anisotropy and the stress direction remain unchanged, K stays at its original value. But according to equation (15) $\boldsymbol{n}^L : \boldsymbol{n}^F$ may change its sign (e.g. from positive to negative), resulting in a very large value for $k[1 - (\boldsymbol{n}^L : \boldsymbol{n}^F)\phi]$ such that $\theta > 0$ and $D > 0$. This may naturally lead to cyclic contraction.

Non-coaxiality

The new findings may also facilitate the modelling of non-coaxiality between the stress and the plastic strain

increment, as observed by Gutierrez *et al.* (1993), Yoshimine *et al.* (1998) and others. The plastic strain increment is defined according to the associated flow rule

$$\mathrm{d}\varepsilon_{ij}^{\mathrm{p}} = \langle \mathrm{d}L \rangle \frac{\partial f}{\partial \sigma_{ij}} \tag{18}$$

where $\langle \mathrm{d}L \rangle$ denotes a non-negative loading multiplier. Assume a fabric-dependent yield function with the form

$$f = f(\sigma_{ij}, F_{ij}, H, K) \tag{19}$$

where H is a hardening parameter. The use of equation (19) in equation (18) leads to

$$\begin{aligned} \mathrm{d}\varepsilon_{ij}^{\mathrm{p}} &= \langle \mathrm{d}L \rangle \frac{\partial f}{\partial \sigma_{ij}} \\ &= \langle \mathrm{d}L \rangle \left(\frac{\partial \bar{f}}{\partial \sigma_{ij}} + \frac{\partial f}{\partial K} \frac{\partial K}{\partial \sigma_{ij}} \right) \end{aligned} \tag{20}$$

where $\bar{f}$ denotes the terms in the yield function without the involvement of K. The second term in the right-hand bracket of equation (20), $(\partial f/\partial K)(\partial K/\partial \sigma_{ij})$, may account for the non-coaxial behaviour observed in granular materials. A rather significant difference between the fabric orientation and the loading direction in the early stage of loading may induce this term to deviate substantially from the stress direction, thus contributing to the overall non-coaxial plastic strain increment. At a relatively large strain level, when σ_{ij} and F_{ij} become coaxial and compatible with each other, this term will become more coaxial with σ_{ij}, as will the overall plastic strain increment $\mathrm{d}\varepsilon_{ij}^{\mathrm{p}}$ with respect to σ_{ij}.

Other relevant issues

There are other noteworthy issues relevant to the observations found in the study, including *initial anisotropy*, *particle crushing* and *strain localisation*. All the observations presented so far have been based on consideration of initially isotropic sand samples. The influence of initial (or inherent) anisotropy can be investigated further using non-spherical DEM particles. Nevertheless, it is believed that the shearing process will totally destroy all previous memories of granular media, including initial anisotropy, such that the critical state will not be affected by the initial state (see also Yimsiri & Soga, 2010). Meanwhile, real experimental tests on sand involve some level of particle crushing, which was not considered in this study. It is expected, however, that significant particle crushing will lead to an essentially quite different material in the final stage from that at the beginning. Hence it is irrelevant to discuss the uniqueness of the critical state in this case. Regarding strain localisation, this effect has rarely been observed in the present authors' DEM simulations, probably because of the use of rigid walls and free-rolling particles. It remains arguable whether it is still valid to discuss the critical state as being homogeneous, as envisaged by Roscoe *et al.* (1958), in the presence of strain localisation in a soil sample.

CONCLUSIONS

Motivated by the anisotropic critical state theory recently proposed by Li & Dafalias (2012), this study explored the characteristics of critical states in granular materials under the influence of fabric anisotropy. Using a 3D DEM, granular assemblies with different initial void ratios and confining pressures were sheared to a critical state under both drained and undrained loading conditions, and with different intermediate principal stress ratios. A number of novel observations were identified from the results.

(*a*) The critical state in granular media can be uniquely characterised. Rather than referring to an isotropic state, it is always associated with a fabric structure compatible with the critical stress state.
(*b*) The critical fabric anisotropy is not unique, but depends on the specific loading path. It is strongly related to the critical stress state, and cannot be separated as an individual or unique reference for the soil state.
(*c*) The first joint invariant of the stress tensor and the fabric tensor, K, is uniquely related to the pressure level at critical state, and the correlation is path-independent.
(*d*) The correlations among K, e and p' at critical state can be visualised by a unique spatial critical state curve in K–e–p' space. The projection of this curve onto the e–p' plane is the critical state line defined by classic critical state theory. A new definition of the critical state is proposed by incorporating the additional unique condition of K_{c}.
(*e*) The critical K_{c} can be further normalised to be a constant that is independent of either the loading path or the pressure level.

In light of the new findings, future challenges and opportunities for the development of theoretical soil mechanics are discussed above, with relevance to such topics as the choice of state parameters, the definition of the dilatancy relation, the modelling of non-coaxiality, and the quantification of the critical state in the presence of strain localisation, particle crushing and initial anisotropy.

NOTATION

A	fabric anisotropic variable used by Li & Dafalias (2012)
A'	measure of relative orientation between fabric and stress direction
A_{c}	critical fabric anisotropic variable used by Li & Dafalias (2012)
b	intermediate principal stress ratio
C	material constant in equations (14) and (17)
D	dilatancy
d	material constant in equations (14) and (17)
$\boldsymbol{d}^{\mathrm{c}}$, d_i^{c}	branch vector and its component in the ith direction
$E(\Theta)$	contact normal probability density function
e	void ratio
e_{c}	critical void ratio
e_Γ	critical void ratio at zero pressure
F	degree of fabric anisotropy
F_{c}	critical fabric anisotropy
F_{ij}	deviatoric fabric tensor
f	yield function
$\boldsymbol{f}^{\mathrm{c}}$, f_i^{c}	contact force vector and its component in the ith direction
H	hardening parameter in equation (19)
I_1, $J_{2\mathrm{D}}$, $J_{3\mathrm{D}}$	three invariants of stress tensor
I_1^{F}, I_2^{F}, I_3^{F}	three invariants of original fabric tensor ϕ_{ij}
J_1^{F}, J_2^{F}, J_3^{F}	three invariants of deviatoric fabric tensor F_{ij}
K (K_1), K_2, K_3, K_4	four joint invariants between deviatoric stress tensor and fabric tensor
K_{c}	critical fabric anisotropy parameter
k	material constant in equation (13)
k_{n}, k_{s}	normal and tangential stiffness
$\langle \mathrm{d}L \rangle$	non-negative loading multiplier
$M(\eta_{\mathrm{c}})$	critical stress ratio
m	material constant in equations (14) and (17)
m_{F}	material parameter in equation (8)
N_{c}	total contact number within volume
$\boldsymbol{n}$, n_i	unit contact normal vector and its component in the ith direction

$\boldsymbol{n}^{\mathrm{F}}$ unit tensor denoting the fabric direction in equation (15)
$\boldsymbol{n}^{\mathrm{L}}$ unit tensor denoting the loading direction in equation (15)
n_{ij}^{F} unit-norm deviatoric fabric tensor used by Li & Dafalias (2012)
n_{ij}^{s} unit-norm deviatoric stress tensor used by Li & Dafalias (2012)
p' mean effective stress
p_{a} atmospheric pressure
q deviatoric stress
r^2 regression coefficient of determination
s_{ij} deviatoric stress tensor
V sample volume
α material constant in equation (11)
δ exponent in power law for fitting q–p' at critical state
δ_{ij} Kronecker delta
ε_1 accumulated axial strain
$\mathrm{d}\varepsilon_{ij}^{\mathrm{p}}$ plastic strain increment
ζ material parameter in equation (8)
η stress ratio
η^* Lade-like scalar function of I_1^{F}, I_2^{F} and I_3^{F}
θ overall state parameter
λ_{e} material constant in equation (7)
ξ material constant in equation (7)
σ_1, σ_2, σ_3 the three principal stresses
σ_{ij} stress tensor
ϕ anisotropic state parameter
ϕ_{ij} fabric tensor
ψ isotropic state parameter

ACKNOWLEDGEMENTS

The authors wish to thank Professors Xiang-song Li and Yannis Dafalias for making a preprint of their work (Li & Dafalias, 2012) available to us. They are also grateful to Professor Xiang-song Li and Professor Niels Kruyt for the numerous stimulating discussions. The study was financially supported by a GRF grant of Research Grants Council of Hong Kong (Project No. 622910).

REFERENCES

Abe, S., Place, D. & Mora, P. (2004). A parallel implementation of the lattice solid model for the simulation of rock mechanics and earthquake dynamics. *Pure Appl. Geophys*. **161**, No. 11–12, 2265–2277.

Baji, K. (1996). Stress and strain in granular assemblies. *Mech. Mater.* **22**, No. 3, 165–177.

Barreto, D. & O'Sullivan, C. (2012). The influence of inter-particle friction and the intermediate stress ratio on soil response under generalized stress conditions. *Granular Matter* **14**, No. 4, 505–521.

Been, K. & Jefferies, M. G. (1985). A state parameter for sands. *Géotechnique* **35**, No. 2, 99–112, http://dx.doi.org/10.1680/geot.1985.35.2.99.

Been, K., Jefferies, M. G. & Hachey, J. (1991). The critical state of sands. *Géotechnique* **41**, No. 3, 365–381, http://dx.doi.org/10.1680/geot.1991.41.3.365.

Christoffersen, J., Mehrabadi, M. M. & Nemat-Nasser, S. (1981). A micromechanical description of granular material behavior. *J. Appl. Mech. ASME* **48**, No. 2, 339–344.

Guo, N. & Zhao, J. (2013). Signature of anisotropy in granular materials under shear. *Comput. Geotech*. **47**, 1–15.

Gutierrez, M., Ishihara, K. & Towhata, I. (1993). Flow theory for sand during rotation of principal stress direction. *Soils Found*. **31**, No. 4, 121–132.

Hall, S. A., Bornert, M., Desrues, J., Pannier, Y., Lenoir, N., Viggiani, G. & Bésuelle, P. (2010). Discrete and continuum experimental study of localized deformation in Hostun sand under triaxial compression using X-ray μCT and 3D digital image correlation. *Géotechnique* **60**, No. 5, 315–322, http://dx.doi.org/10.1680/geot.2010.60.5.315.

Hasan, A. & Alshibli, K. A. (2010). Experimental assessment of 3D particle-to-particle interaction within sheared sand using synchrotron microtomography. *Géotechnique* **60**, No. 5, 369–379, http://dx.doi.org/10.1680/geot.2010.60.5.369.

Hasan, A. & Alshibli, K.A. (2012). Three dimensional fabric evolution of sheared sand. *Granular Matter* **14**, No. 4, 469–482.

Ishihara, K. (1993). Liquefaction and flow failure during earthquakes. *Géotechnique* **43**, No. 3, 351–415, http://dx.doi.org/10.1680/geot.1993.43.3.351.

Ishihara, K., Tatsuoka, F. & Yasuda, S. (1975). Undrained deformation and liquefaction of sand under cyclic stresses. *Soils Found*. **15**, No. 1, 29–44.

Jefferies, M. G. & Been, K. (2006). *Soil liquefaction: A critical state approach*. London, UK: Taylor & Francis.

Kanatani, K. (1984). Distribution of directional data and fabric tensors. *Int. J. Engng Sci*. **22**, No. 2, 149–164.

Li, X. & Li, X. S. (2009). Micro-macro quantification of the internal structure of granular materials. *J. Engng Mech. ASCE* **135**, No. 7, 641–656.

Li, X. S. (1997). Modeling of dilative shear failure. *J. Geotech. Geoenviron. Engng ASCE* **123**, No. 7, 609–616.

Li, X. S. & Dafalias, Y. F. (2000). Dilatancy for cohesionless soils. *Géotechnique* **50**, No. 4, 449–460, http://dx.doi.org/10.1680/geot.2000.50.4.449.

Li, X. S. & Dafalias, Y. F. (2012). Anisotropic critical state theory: the role of fabric. *J. Engng Mech. ASCE* **138**, No. 3, 263–275.

Li, X. S., Dafalias, Y. F. & Wang, Z.-L. (1999). State-dependent dilatancy in critical-state constitutive modeling of sand. *Can. Geotech. J.* **36**, No. 4, 599–611.

Masson, S. & Martinez, J. (2001). Micromechanical analysis of the shear behavior of a granular material. *J. Engng Mech. ASCE* **127**, No. 10, 1007–1016.

Mueth, D. M., Debregeas, G. F., Karczmar, G. S., Eng, P. J., Nagel, S. R. & Jaeger, H. M. (2000). Signatures of granular microstructure in dense shear flows. *Nature* **406**, No. 6794, 385–389.

Nakata, Y., Hyodo, M., Murata, H. & Yasufuku, N. (1998). Flow deformation of sands subjected to principal stress rotation. *Soils Found*. **38**, No. 2, 115–128.

Ng, T., Aube, D. & Altobelli, S. (1997). 3-D MRI experiment of granular materials. In *Proceedings of symposium on mechanical deformation and flow of particulate materials*, Evanston, IL, pp. 189–198.

Oda, M. (1972a). Initial fabrics and their relations to mechanical properties of granular material. *Soils Found*. **12**, No. 1, 17–36.

Oda, M. (1972b). The mechanism of fabric changes during compressional deformation of sand. *Soils Found*. **12**, No. 2, 1–18.

Oda, M. (1982). Fabric tensor for discontinuous geological materials. *Soils Found*. **22**, No. 4, 96–108.

Oda, M., Nemat-Nasser, S. & Konishi, J. (1985). Stress-induced anisotropy in granular masses. *Soils Found*. **25**, No. 3, 85–97.

Ouadfel, H. & Rothenburg, L. (2001). 'Stress–force–fabric' relationship for assemblies of ellipsoids. *Mech. Mater.* **33**, No. 4, 201–221.

Roscoe, K. H., Schofield, A. N. & Wroth, C. P. (1958). On the yielding of soils. *Géotechnique* **8**, No. 1, 22–53, http://dx.doi.org/10.1680/geot.1958.8.1.22.

Roscoe, K. H., Schofield, A. N. & Thurairajah, A. (1963). Yielding of clays in states wetter than critical. *Géotechnique* **13**, No. 3, 211–240, http://dx.doi.org/10.1680/geot.1963.13.3.211.

Rothenburg, L. & Bathurst, R. J. (1989). Analytical study of induced anisotropy in idealized granular materials. *Géotechnique* **39**, No. 4, 601–614, http://dx.doi.org/10.1680/geot.1989.39.4.601.

Satake, M. (1982). Fabric tensor in granular materials. In *Deformation and failure of granular materials* (eds P. A. Vermeer and H. J. Luger), pp. 63–68. Rotterdam, the Netherlands: Balkema.

Schofield, A. N. & Wroth, C. P. (1968). *Critical state soil mechanics*. London, UK: McGraw-Hill.

Spencer, A. J. M. (1971). Theory of invariants. In *Continuum physics I* (Part III) (ed. A. C. Eringen), pp. 239–353. New York, NY, USA: Academic Press.

Thornton, C. (2000). Numerical simulations of deviatoric shear deformation of granular media. *Géotechnique* **50**, No. 1, 43–53, http://dx.doi.org/10.1680/geot.2000.50.1.43.

Thornton, C. & Zhang, L. (2010). On the evolution of stress and

microstructure during general 3D deviatoric straining of granular media. *Géotechnique* **60**, No. 5, 333–341, http://dx.doi.org/10.1680/geot.2010.60.5.333.
Verdugo, R. & Ishihara, K. (1996). The steady state of sandy soils. *Soils Found.* **36**, No. 2, 81–92.
Wang, C.-C. (1970). A new representation theorem for isotropic functions. *Arch. Ration. Mech. Anal*. **36**, No. 3, 166–197.
Yimsiri, S. & Soga, K. (2010). DEM analysis of soil fabric effects on behaviour of sand. *Géotechnique* **60**, No. 6, 483–495, http://dx.doi.org/10.1680/geot.2010.60.6.483.
Yoshimine, M., Ishihara, K. & Vargas, W. (1998). Effects of principal stress direction and intermediate principal stress on undrained shear behavior of sand. *Soils Found*. **38**, No. 3, 179–188.